J|A|C|S
COMMUNICATIONS

Published on Web 03/18/2006

In situ Synthesis of Mixed-Valent Manganese Oxide Nanocrystals: An In situ Synchrotron X-ray Diffraction Study

Xiong-Fei Shen,[†] Yun-Shuang Ding,[†] Jonathan C. Hanson,[‡] Mark Aindow,[†] and Steven L. Suib*[,†,§,¶]

Institute of Materials Science, Department of Chemistry, and Department of Chemical Engineering, University of Connecticut, 55 North Eagleville Road, Storrs, Connecticut 06269, and Department of Chemistry, Brookhaven National Laboratory, Upton, New York 11973

Received December 13, 2005; E-mail: steven.suib@uconn.edu

Porous mixed-valent manganese oxides are a group of multifunctional materials which can be used as molecular sieves, catalysts, battery materials, and gas sensors.[1] Natural mineral manganese oxides are widely available; however, their structures and properties usually are not uniform, and thus their activities are not reproducible. Therefore, various methods have been developed to synthesize manganese oxides with more uniform structures/properties.[2] However, material properties and thus activity can vary significantly with different synthesis methods or even with the same synthesis method but different conditions, such as synthesis temperature and time. Therefore, for better control of the property and activity of materials, kinetic and mechanistic information of structure changes during synthesis should be known to provide feedback for the optimized design of materials.

Classical studies of phase transformation kinetics and mechanism are usually carried out in an ex situ mode. That is, materials need to be isolated out from the synthesis mixtures and followed by washing/drying before they can be characterized for structural/phase information. In such a way, the materials actually may not be the same as they are in the synthesis system. Therefore, in situ characterizations are desired. The development of synchrotron radiation has provided opportunities for studying the structures and properties of materials in an efficient in situ way due to its high energy flux (e.g., a good XRD pattern can be obtained in a 1 min scan). Therefore, in situ studies of structure and property changes with pressures and temperature are possible for materials, such as zeolites, steel, carbon nanotubes, Cu/CuO, and polymers.[3,4] However, most reported in situ synchrotron XRD studies are focused on solid state/gel systems by measuring phase changes during pressure or heat treatment. Phase transformations during material synthesis and their applications, especially in wet/solution chemistry processes in different media, have not drawn much attention.

Here, we report the study of phase transformations during hydrothermal syntheses by in situ synchrotron powder XRD using manganese oxides as examples. Synthesis of β-MnO_2 is used as a typical example to illustrate how phase changes in a wet chemistry (acidic conditions) and pressurized process can be resolved by in situ synchrotron XRD. More examples are also given to illustrate in situ studies of neutral and basic wet chemistry processes under pressurized conditions. Examples for application of the in situ study results in material design are also given.

In the synthesis of β-MnO_2, dried birnessite (NaOL-1), a layered structure manganese oxide, was mixed with 1 M HNO_3 solution to form a slurry. The slurry was injected into a quartz capillary tube, which was used as the hydrothermal synthesis reactor. The only open-end of the quartz tube was connected to the goniometer with Swagelok fittings and was sealed by back-pressure gas (air) to prevent the vaporization of water (i.e., to imitate the hydrothermal conditions).[4d] Heating was realized by flowing heated air underneath the tube. The time-resolved XRD patterns are shown in Figure 1 (5 min/scan). After ~10 scans, the disappearance of the (002) diffraction peak for the NaOL-1 precursor (c direction is the interlayer direction) indicates the loss of the NaOL-1 layered structure. After ~20 scans, β-MnO_2 phase starts to form.

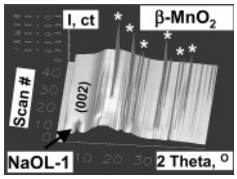

Figure 1. In situ synchrotron XRD patterns for synthesis of a β-MnO_2 (1×1 tunnel structure) by hydrothermal treatment of NaOL-1 with 1 M HNO_3. The system was heated from 25 to 180 °C at 6.2 °C/min, and held at 180 °C. XRD patterns were collected continuously with 5 min/pattern (λ = 0.922 Å, beamline X7B, NSLS, BNL).

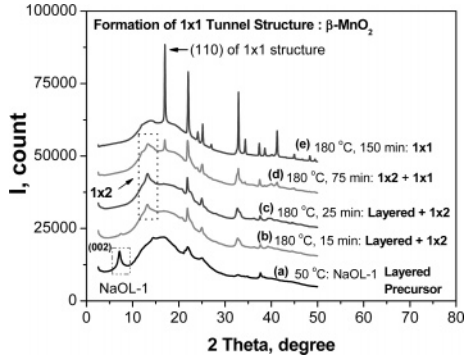

Figure 2. XRD patterns at different stages: (a) 50 °C, NaOL-1 is the only phase; (b) 180 °C, 15 min, layered structure + 1×2 tunnel structure; (c) 180 °C, 25 min, layered structure (compressed) + 1×2 tunnel structure; (d) 180 °C, 75 min, $1 \times 1 + 1 \times 2$ (dominant) tunnel structures; (e) 180 °C, 150 min, 1×1 tunnel structure only. (The broad bump at 2θ between 20 and 30° is due to the quartz tube.)

Details of the process are illustrated by plotting the individual patterns at different stages, as shown in Figure 2. After 15 min at 180 °C, the (002) diffraction peak of NaOL-1 almost disappears, while other diffraction peaks are still present. This indicates that the layer structure of NaOL-1 was modified to a smaller interlayer spacing due to compression in the c direction of NaOL-1.

At the same time, the characteristic diffraction peak for the 1×2 tunnel structure manganese oxide (ramsdellite), the (101) plane diffraction at $2\theta \approx 14°$, starts to appear. This indicates that, accompanied with the layer compression, closing up of layers occurs simultaneously to form tunnel structures. At this stage, original and compressed layered structures and 1×2 tunnel structures coexist.

[†] Institute of Materials Science, University of Connecticut.
[‡] Brookhaven National Laboratory.
[§] Department of Chemistry, University of Connecticut.
[¶] Department of Chemical Engineering, University of Connecticut.

10.1021/ja058456+ CCC: $33.50

Scheme 1. Schematic of the Phase Transformation Mechanism from Layered Structure to Tunnel Structure Manganese Oxides under Hydrothermal Conditions

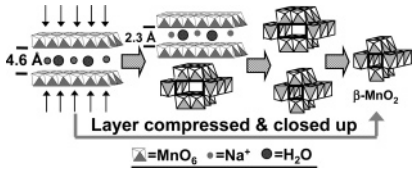

At 180 °C from 25 to 75 min, more compressed layers were transformed into the 1 × 2 tunnel structure. After 75 min, some 1 × 2 tunnel structures start to transform to the 1 × 1 tunnel structure (β-MnO_2) as indicated by the occurrence of the diffraction peak for (110) planes of β-MnO_2 at $2\theta \approx 17°$. At these stages, 1 × 1 and 1 × 2 tunnel structures coexist. After 150 min at 180 °C, only 1 × 1 tunnel structure is present. Transformation from NaOL-1 layered precursor to 1 × 1 tunnel structure, β-MnO_2, is completed. The phase transformation process is illustrated in Scheme 1, [NaOL-1 layered precursor] to [compressed layered structure + 1 × 2 tunnel structure] to [1 × 2 + 1 × 1 tunnel structures] and then to [1 × 1 tunnel structure].

On the basis of the phase transformation mechanism, syntheses were made in these different stages. The morphologies of the produced phases are shown in Figure 3. NaOL-1 shows a typical plate morphology for layered structure materials. After the structure starts to transform to the 1 × 2 tunnel structure, a nanofiber/nanorod morphology is formed, which is typical for tunnel structure manganese oxides. Further treatment under acidic conditions leads to the complete transformation to the 1 × 1 tunnel structure and the reduction of aspect ratios of the rods due to an "acid etching effect".[2c] Interestingly, the produced β-MnO_2 shows a hollow nanocrystal morphology, as shown in Figure 3d. The reasons why the hollow morphology is formed is not yet completely understood. Crystal micro-twining could be one of the reasons.

Two more examples were studied in a similar in situ synchrotron XRD manner, except that a sapphire capillary tube was used as the reactor since the quartz capillary tube is too brittle at high pressure/basic conditions. Figure 4a shows the direct hydrothermal transformation of the MnOOH precursor to a pure KOMS2 phase (a 2 × 2 tunnel structure manganese oxide) within 10 min at 120 °C. Figure 4b shows the transformation of NaOL-1 at 1 M NaOH, 180 °C hydrothermal conditions, to a 2 × 4 tunnel structure manganese oxide. Only two phases were observed, indicating no other immediate phases were involved during synthesis. One example for optimization of material synthesis after knowing the phase transformation mechanism is that the KOMS2 phase was obtained for hydrothermal treatment of a MnOOH precursor at 120 °C for 10 min, 20 min, and 12 h, respectively, which produces material with BET surface areas of 160, 77, and 70 m^2/g,

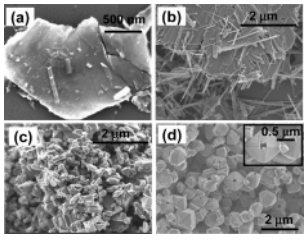

Figure 3. Electron microscope images of materials during the hydrothermal synthesis of β-MnO_2. (a) NaOL-1 precursor showing a plate morphology. (b) Formation of a 1 × 2 tunnel structure, plate starts to dissemble and form rods. (c) Mixtures of 1 × 1 and 1 × 2 tunnel structures, nanorod morphology, (d) hollow nanocrystal of β-MnO_2 (inset shows a typical tetragonal hollow crystal with a lateral length of ~700 nm and a hole diameter of ~100 nm).

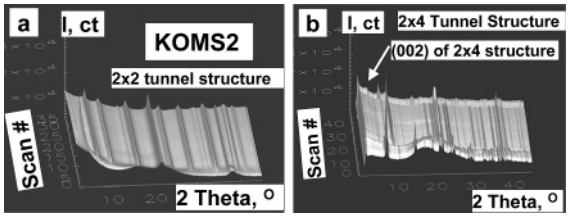

Figure 4. Phase transformations during in situ synthesis studied by in situ synchrotron XRD. (a) Formation of a KOMS2 phase by hydrothermal treatment of MnOOH with H_2O at 120 °C. (b) Formation of a 2 × 4 tunnel structure manganese oxide by hydrothermal treatment of NaOL-1 precursor with 1 M NaOH at 180 °C (λ = 0.922 Å, 5 min/scan).

respectively (usually KOMS2 is obtained after 12−24 h hydrothermal treatment in this synthesis method). Therefore, the surface area can be maximized/controlled for the same pure crystal phase.

In summary, we have demonstrated the successful in situ characterizations of phase transformations by in situ synchrotron powder X-ray diffraction for wet chemistry systems at different pH media. Quartz capillary tubes are brittle for high temperature/basic systems. The sapphire capillary tube is robust for pressurized, acidic, and basic conditions. In situ synchrotron XRD studies provide an opportunity for better control of material syntheses, which is difficult to achieve for conventional kinetic study methods as also suggested by others.[4] For example, different surface areas for a pure KOMS2 phase and varying tunnel structures of manganese oxides can be controlled in studies here. This method is not limited to manganese oxides but can be used for in situ characterization of other materials during synthesis using hydrothermal, sol−gel, or other methods. In addition, catalytic processes in liquid−solid, gas−solid, or solid−solid systems can also be studied in an in situ way. Combined with Rietveld refinement, oxygen/cation vacancies or defects in the catalyst structure can be investigated for a better understanding of the catalytic mechanisms. As a result, catalyst synthesis and catalytic processes can be optimized.

Acknowledgment. We thank Dr. F. Galasso for advice and the Geosciences and Biosciences Division, Office of Basic Energy Sciences, Office of Science, U.S. Department of Energy for financial support under Contract No. AC02-98CH10086.

Supporting Information Available: Experiments, XRD patterns, and SEM images for the 2 × 2 and 2 × 4 tunnel structures. This material is available free of charge via the Internet at http://pubs.acs.org.

References

(1) (a) Bish, D. L.; Post, J. E. *Am. Mineral.* **1989**, *74*, 177. (b) Shen, Y. F.; Zerger, R. P.; DeGuzman, R. N.; Suib, S. L.; Macurdy, L.; Potter, D. I.; O'Young, C. L. *Science* **1993**, *260*, 511. (c) Giraldo, O.; Brock, S. L.; Marquez, M.; Suib, S. L.; Hillhouse, H.; Tspatsis, M. *Nature* **2000**, *405*, 38. (d) Boukamp, A. A. *Nat. Mater.* **2003**, *2*, 294. (e) Ma, R.; Bando, Y.; Zhang, L.; Sasaki, T. *Adv. Mater.* **2004**, *16*, 918.

(2) (a) Turner, S.; Post, J. E. *Am. Mineral.* **1988**, *73*, 1155. (b) Kim, J.; Manthiram, A. *Nature* **1997**, *390*, 165. (c) Shen, X. F.; Ding, Y. S.; Liu, J.; Cai, J.; Laubernds, K.; Zerger, R. P.; Vasilev, A.; Aindow, M.; Suib, S. L. *Adv. Mater.* **2005**, *17*, 805.

(3) (a) Lee, Y.; Vogt, T.; Hriljac, J. A.; Parise, J. B.; Hanson, J. C.; Kim, S. J. *Nature* **2002**, *420*, 485. (b) Offerman, S. E.; Van Dijk, N. H.; Sietsma, J.; Grigull, S.; Lauridsen, E. M.; Margulies, L.; Poulsen, H. F.; Rekveldt, M. Th.; Van der Zwaag, S. *Science* **2002**, *298*, 1003. (c) Rodriguez, J. A.; Hanson, J. C.; Frenkel, A. I.; Kim, J. Y.; Perez, M. *J. Am. Chem. Soc.* **2002**, *124*, 346. (d) Eastman, J. A.; Fuoss, P. H.; Rehn, L. E.; Baldo, P. M.; Zhou, G.-W.; Fong, D. D.; Thompson, L. J. *Appl. Phys. Lett.* **2005**, *87*, 051914/1.

(4) (a) Norby, P.; Hanson, J. C. *Catal. Today* **1998**, *39*, 301. (b) Loiseau, T.; Beitone, L.; Millange, F.; Taulelle, F.; O'Hare, D.; Ferey, G. *J. Phys. Chem. B* **2004**, *108*, 20020. (c) Cahill, C. L.; Benning, L. G.; Barnes, H. L.; Parise, J. B. *Chem. Geo.* **2000**, *167*, 53. (d) Dmitri, G. M.; Tripathi, A.; Clearfield, A.; Celestian, A. J.; Parise, J. B.; Hanson, J. C. *Chem. Mater.* **2004**, *16*, 3659.

JA058456+